Available online at www.sciencedirect.com
ScienceDirect
Ceramics International 37 (2011) 2359–2364
CERAMICS INTERNATIONAL
www.elsevier.com/locate/ceramint

Low-temperature preparation of lanthanum-doped $BiFeO_3$ crystallites by a sol–gel-hydrothermal method

Zhiwu Chen [a,b,d,*], Jianqiang Hu [b,c], Zhenya Lu [a], Xinhua He [a]

[a] College of Materials Science and Engineering, South China University of Technology, Guangzhou 510640, PR China
[b] State Key Laboratory of Pulp and Paper Engineering, South China University of Technology, Guangzhou 510640, PR China
[c] College of Chemistry and Chemical Engineering, South China University of Technology, Guangzhou 510640, PR China
[d] State Key Laboratory of Advanced Technology for Materials Synthesis and Processing, Wuhan University of Technology, Wuhan 430070, PR China

Received 30 August 2010; received in revised form 4 January 2011; accepted 21 March 2011
Available online 1 June 2011

Abstract

Multiferroic $Bi_{1-x}La_xFeO_3$ (BLFO, $x = 0, 0.15, 0.3, 0.4$) powders were for the first time synthesized by a novel sol–gel-hydrothermal route. The as-prepared samples were characterized by X-ray diffraction (XRD), scanning electron microscopy (SEM), and fourier transform infrared (FT-IR) spectroscopy. The XRD results indicated that pure BLFO crystallites could be obtained for $x \leq 0.3$, and the phase purity was sensitive to the concentration of mineralizer. SEM results revealed that the morphology and dimension of the BLFO microspheres and submicrotiles could be effectively controlled by varying KOH concentrations. The formation mechanism of the BLFO crystalline was also discussed.

Keywords: $BiFeO_3$; Sol–gel-hydrothermal; Lanthanum doping; Powder

1. Introduction

Multiferroic materials, which are simultaneously ferroelectric, ferromagnetic, and ferroelastic in the same material, have a wide range of potential applications in information storage, spintronic devices, and sensors [1–3]. As one of the representative single-phase multiferroics, $BiFeO_3$ (BFO) is extensively studied because of its high ferroelectric Curie temperature ($T_C \approx 820\ ^\circ C$) and high antiferromagnetic Néel temperature ($T_N \approx 370\ ^\circ C$) [4]. However, a superimposed spiral spin structure with an incommensurate long-wavelength period of 62 nm cancels macroscopic magnetization and also inhibits linear magnetoelectric effect in bulk $BiFeO_3$ [5]. The other obstacle for $BiFeO_3$ applications is large leakage current because of the existence of the second phase. Due to the complex phase diagram of Bi_2O_3–Fe_2O_3, with $Bi_2Fe_4O_9$ and $Bi_{25}FeO_{40}$ being the stable compounds surrounding $BiFeO_3$ [6], it is difficult to obtain a single phase multiferroic $BiFeO_3$ through conventional solid-state reaction at high sintering temperature [7,8]. In order to overcome these disadvantages, many attempts have been done recently, which include: (i) doping rare-earth (Re) or transition metal (Tm) elements into Bi or Fe sites to increase phase stability of $BiFeO_3$ [9,10]; (ii) synthesizing $BiFeO_3$ nanoparticle with grain size below 62 nm to achieve ferromagnetism by destroying spiral spin structure [11]; and (iii) several alternative chemical synthesis routes, such as the ferrioxalate precursor method [9], co-precipitation method [12], the soft chemical route [13], microemulsion technique [14], sol–gel process [15], polymeric precursor method [16] and so on, have been proposed to synthesize single phase $BiFeO_3$ or BLFO. However, these chemical methods still need an additional calcined process at $>400\ ^\circ C$, which is far from low cost and results in irregular morphology and broad distribution of particle sizes. Nevertheless, among these approaches, partial substitution of A-site (Bi^{3+}) by rare earth element ions improves the phase purity, and thus enhances electrical and magnetic properties. The stability of lanthanum and the collapse of cycloidal spin structure of BFO by A-site substitution with lanthanum significantly improve its multiferroic properties [9,10].

The sol–gel-hydrothermal processing represents an alternative to the calcinations for the crystallization of an objective

* Corresponding author at: College of Materials Science and Engineering, South China University of Technology, Guangzhou 510640, China.
Tel.: +86 20 22236602; fax: +86 20 22236602.
E-mail address: chenzw@scut.edu.cn (Z. Chen).

0272-8842/$36.00
doi:10.1016/j.ceramint.2011.03.081

compound under mild temperatures. As a novel method to prepare oxide powders, the sol–gel-hydrothermal technique has the advantages of both sol–gel and hydrothermal syntheses and has attracted extensive attentions due to its high degree of crystallinity, well-controlled morphology, high purity, and narrow particle size distribution [17,18].

In the present work, the sol–gel-hydrothermal process was presented as a new route to produce $Bi_{1-x}La_xFeO_3$ ($x = 0$, 0.15, 0.3, 0.4) powders at a temperature below 200 °C, which is much lower than that synthesized by the normal sol–gel route. The influence of the hydrothermal condition on the crystal structure and the morphology of BLFO powders were investigated, and the formation mechanism of the BLFO powders was also discussed.

2. Experimental procedure

The raw materials used in the present work were analytical grade, such as bismuth nitrate pentahydrate ($Bi(NO_3)_3{\cdot}5H_2O$), lanthanum nitrate ($La(NO_3)_3{\cdot}6H_2O$), iron nitrate ($Fe(NO_3)_3{\cdot}9H_2O$), potassium hydroxide (KOH), glacial acetic acid and ethylene alcohol. Firstly, $Bi(NO_3)_3{\cdot}5H_2O$ and $La(NO_3)_3{\cdot}6H_2O$ were dissolved into glacial acetic acid, and ethylene alcohol was added under stirring after the solution became transparent. The mixture was then introduced into the prepared solution of a stoichiometric amount of $Fe(NO_3)_3{\cdot}9H_2O$ in glacial acetic acid. After stirring vigorously for 2 h, a homogeneous, transparent, blackish red, and clear sol was formed. In the sol, we observed Tyndall phenomenon. A stable sol was obtained when the concentration of the precursor was adjusted to 0.2 M by adding acetic acid and ethylene alcohol. It is well known that bismuth nitrate pentahydrate and iron nitrate were easy to hydrolyze in the solution. Glacial acetic acid as the catalyst in the sol system could control the hydrolysis speed and adjust the solution concentration. While ethylene glycol as solvent can keep the different electronegativities of bismuth and iron during hydrolysis and its linearly structured molecule makes it easy to obtain a stable sol [15]. Then the sol was dried at 80 °C to obtain a dry gel. The obtained gel precursor was added into KOH solution for forming a suspension. KOH concentrations were varied from 3 M to 11 M. The as-prepared mixtures were finally poured into a Teflonlined stainless steel autoclave with a filling capacity of 80%. The hydrothermal treatments were conducted under autogeneous pressure at 180 °C for 16 h. After cooling, the products were filtered, washed with distilled water, and dried at room temperature. For comparison, a part of the gel was calcined at 500 °C for 2 h in air.

Crystalline structures of the BLFO powders were examined using an X-ray diffractometer (XRD, D/Max-3C, Japan) with Cu Kα radiation. The morphologies of the synthesized BLFO particles were observed by a Scanning electron microscopy (LEO 1530 VP, SEM). Infrared spectra were measured by a Nicolet-Nexus 670 FTIR spectrometer from 450 cm^{-1} to 4000 cm^{-1}.

3. Results and discussion

Fig. 1 shows XRD patterns of $Bi_{1-x}La_xFeO_3$ crystallites ($x = 0$, 0.15, 0.3, 0.4) synthesized using 7 M KOH at 180 °C for 16 h, as well as the dry gel. As shown in Fig. 1, no characteristic peaks of BLFO and other phases were detected from the dry gel, indicating that the gel were still in the amorphous state. It revealed that when $x = 0$, 0.15, 0.3, all diffraction peaks of these three XRD patterns were assigned to $BiFeO_3$ as reported in JCPDS file (JCPDS No. 86-1518). The XRD results inferred that La had diffused into the perovskite lattice to form a solid solution, the synthesized powders were single-phase BLFO crystallites and have rhombohedrally distorted perovskite structure with *R*3c at room temperature. While, it was clear that a small amount of impurity-phases $Bi_2Fe_4O_9$ was detected in addition to the major $BiFeO_3$ phase for $x = 0.4$. In addition, the diffraction peaks of BLFO for $x = 0.15$, 0.3, and 0.4 had a slight shift as compared with those of BFO without La, indicating the lattice change caused by the La substitution. This may result from the difference of ionic radius of Bi^{3+} ($r = 1.14$ Å) and La^{3+} ($r = 1.22$ Å) ions. However, the phase structure of BLFO crystallites did not change with increasing La content. It has been reported that BLFO ceramics prepared by the solid state reaction method usually had a structure change from rhombohedral to orthorhombic phase for $x = 0.2$ [19]. The differences of the structure of the BLFO synthesized using the sol–gel-hydrothermal method and the solid state reaction may result from their different preparation processes.

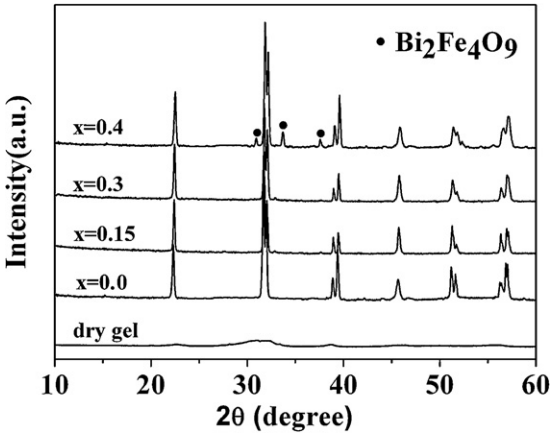

Fig. 1. XRD patterns of $Bi_{1-x}La_xFeO_3$ crystallites ($x = 0$, 0.15, 0.3, 0.4) synthesized using 7 M KOH at 180 °C for 16 h, as well as the dry gel.

The effect of KOH concentration on the formation of BLFO was investigated. Fig. 2 shows XRD patterns of $Bi_{0.7}La_{0.3}FeO_3$ powders synthesized at 180 °C for 16 h using different initial KOH concentrations of 3, 5, 7, 9 and 11 M respectively, as well as powders by a conventional calcination at 500 °C. As shown in Fig. 2, no peaks from lanthana or La-doped impurity phase were detected for all samples, indicating that La have diffused into the perovskite lattice. It was clear that the $Bi_{0.7}La_{0.3}FeO_3$ phase with a perovskite structure was synthesized when the KOH concentrations were 3 M and 5 M, but a small amount of impurity-phases $Bi_2Fe_4O_9$ and $Bi_{25}FeO_{40}$ were also detected. With increasing KOH concentration up to 7 M, the diffraction peaks of the impurity phases disappeared completely. But, further increasing KOH concentration up to 9 M, the $Bi_2Fe_4O_9$ phase appeared again, and a pure $Bi_{0.7}La_{0.3}FeO_3$ phase could be

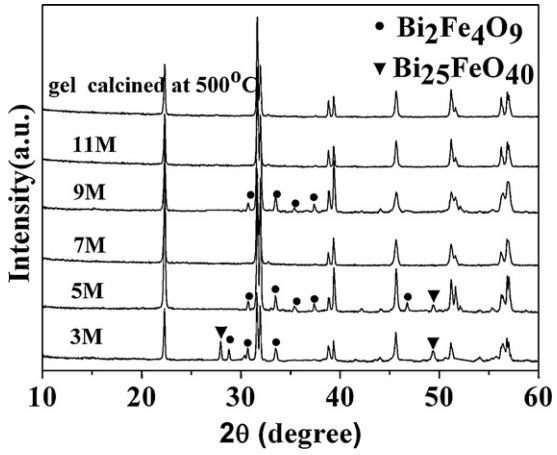

Fig. 2. XRD patterns of $Bi_{0.7}La_{0.3}FeO_3$ powders synthesized using 3, 5, 7, 9, and 11 M KOH (180 °C, 16 h), respectively, as well as powders by a conventional calcination at 500 °C.

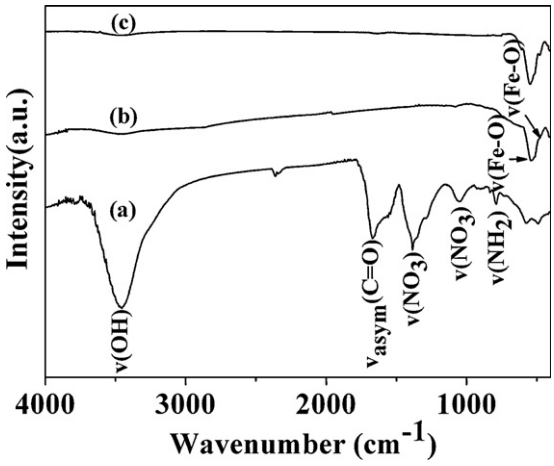

Fig. 3. The IR spectra of (a) gel, (b) $Bi_{0.7}La_{0.3}FeO_3$ powders prepared using 7 M KOH at 180 °C for 16 h, and (c) gel calcined at 500 °C.

obtained in the case of 11 M KOH. It is verified from the above XRD results that pure $Bi_{0.7}La_{0.3}FeO_3$ crystallite could be synthesized when the KOH concentration was 7 and 11 M, possibly indicating that the appropriate amount of KOH was beneficial for the formation of pure BLFO. The as-prepared $Bi_{0.7}La_{0.3}FeO_3$ exhibited a perovskite structure, and the lattice parameters, refined with the MDI Jade 6.5 program are a = 5.625 Å and c = 14.072 Å, which was slightly larger than the literature values of a = 5.582 Å and c = 13.876 Å (JCPDS No. 86-1518). This may result from the difference of Bi^{3+} and La^{3+} ions ionic radius. Meanwhile, it could be seen from Fig. 2 that the features of the two pure BLFO patterns were the same as that of the powders conventionally calcined at 500 °C. However, the synthesizing temperature for pure BLFO powder prepared by the present sol–gel-hydrothermal process was much lower than that of the conventional sol–gel technique. It was evident that the hydrothermal environment remarkably accelerated the reaction kinetics of BLFO.

In order to further analyze the structure changes during the synthesis process, the FT-IR spectra of the dry gel, the $Bi_{0.7}La_{0.3}FeO_3$ powders hydrothermally treated using 7 M KOH at 180 °C for 16 h, and the gel calcined at 500 °C were obtained, respectively, as shown in Fig. 3. The broad band between 3600 cm^{-1} and 3000 cm^{-1} was attributed to O–H stretching [20] originated from ethylene glycol or condensation products, which decreased in intensity in the calcined and hydrothermally synthesized powders, but still persisted, which may be due to the absorption of water molecules from the moisture. The intense band at 1650 cm^{-1} of the dried gel corresponds to the ν_{asym}(C=O) of the co-ordinated oxalate [9], and the bands located at 1385 cm^{-1} and 1050 cm^{-1} indicated the existence of nitrate ions [15]. These peaks disappeared in the calcined and hydrothermally synthesized powders, indicating the removal of carbonates and nitrates. The peak at 804 cm^{-1} of the dry gel was related to NH_2 wagging vibration [15], which also disappeared in the other two powders. The bands between 700 cm^{-1} and 400 cm^{-1} were mainly attributed to the formation of metal oxides. The peaks at 560 and 440 cm^{-1} in the sintered powders assigned to the mode of stretching vibrations along the Fe–O axis and the mode of the Fe–O bending vibration, being characteristics of the octahedral FeO_6 groups in the perovskite compounds [9].

Fig. 4 shows the SEM images of $Bi_{0.7}La_{0.3}FeO_3$ samples synthesized using 5, 7, 9, and 11 M KOH at 180 °C for 16 h. The morphologies of these samples are affected by the concentrations of KOH. When KOH concentration was 5 M, BLFO particles with spheroidal shape were prepared, having a mean diameter of 75 μm. In addition, as shown in left bottom of Fig. 4a, other phases could be found in the sample, which should correspond to the $Bi_2Fe_4O_9$ and $Bi_{25}FeO_{40}$ crystallites shown in XRD pattern (Fig. 2). When KOH concentration was increased to 7 M, the diameter of particles decreased to mean diameter of 25 μm. The smoother surface was obtained compared with the sample prepared using 5 M KOH. However, the particles still retained spheroidal shape (as seen in Fig. 4b). When KOH concentration increased up to 9 M, the particle morphology turned into a tile-shape with a smooth surface. The tile-shaped particles had the side length of about 5 μm and average width of about 2 μm, respectively. In addition, as shown in Fig. 4c, some other phases could be found in the sample, which should correspond to the $Bi_2Fe_4O_9$ crystallites shown in XRD pattern (Fig. 2). Fig. 4d shows SEM image of the BLFO samples obtained at 11 M KOH. The BLFO product still exhibited regular tile-shape morphology, but side length and width of particles were 500 nm and 150 nm, respectively. Such fascinating morphologies of submicrotiles, observed for the first time in BLFO, have not been reported hitherto. Obviously, from the above results, it could be concluded that the morphologies and dimensions of the BLFO samples could be effectively controlled by varying KOH concentrations. In addition, although the XRD patterns of samples synthesized using 7 M and 11 M KOH were similar, the size and morphology of BLFO crystals synthesized under different conditions were completely different, which was consistent with the previously reported literatures [21,22].

The growth mechanism is useful in predicting the growth and evolution of the single crystals. It is believed that the gel

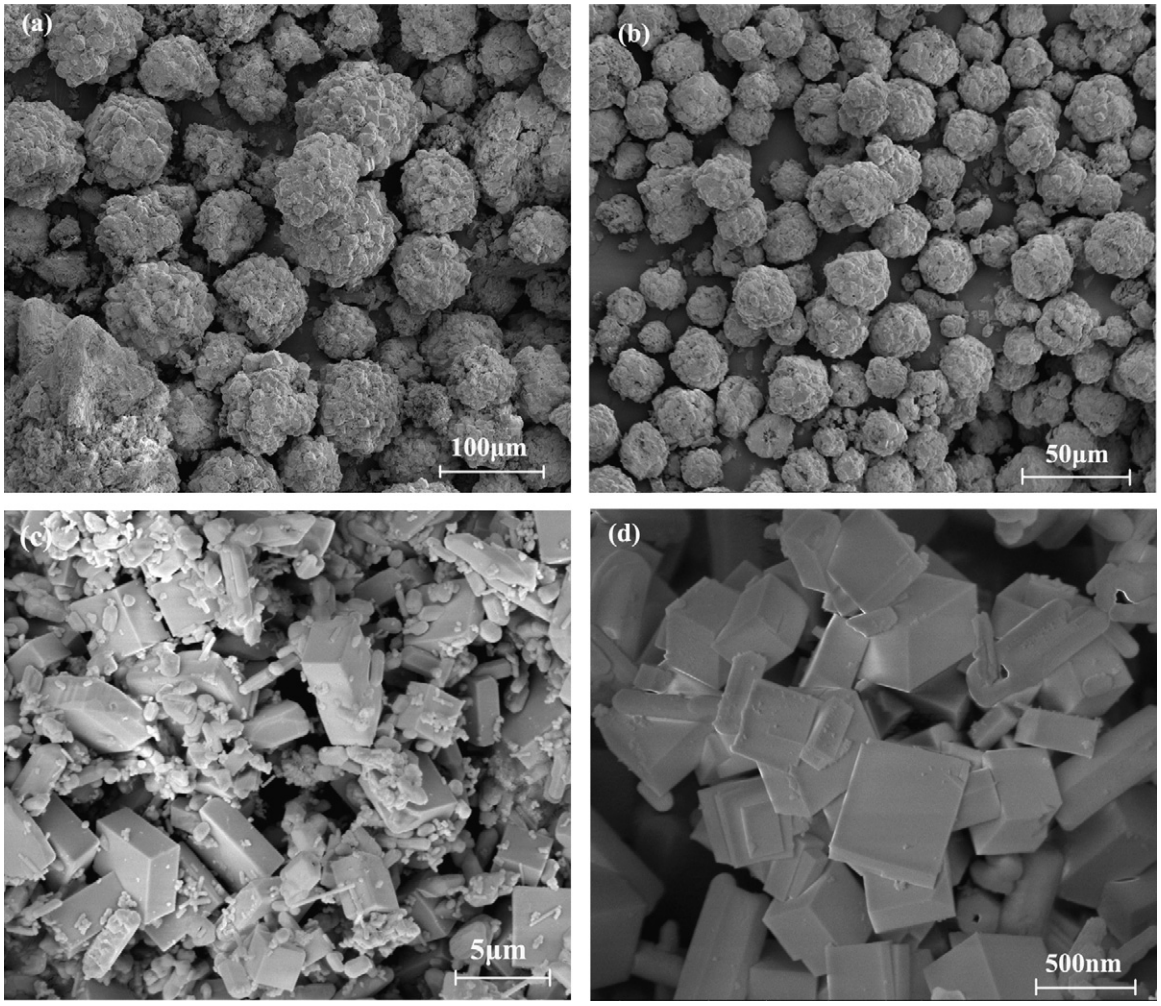

Fig. 4. SEM images of $Bi_{0.7}La_{0.3}FeO_3$ samples synthesized using the KOH concentrations of (a) 5 M, (b) 7 M, (c) 9 M, and (d) 11 M at 180 °C for 16 h.

precursor and hydrothermal environment play a key role in the formation of BLFO crystals. It is supposed that chained nanoclusters with a well defined morphology are formed during the gelation of BLFO sol, by controlling the hydrolysis of the sol. These chained nanoclusters could serve as the nuclei of BLFO during hydrothermal treatment [23]. ''Dissolution–crystallization'' has been considered to be a basic mechanism to describe the hydrothermal process [24,25], in which the dissolution of the reactants is strongly dependent on a mineralizer and crystallization only occurs in the super-saturated fluid. Dissolution takes place when the reactants are loaded and heated in a hydrothermal system; then, more stable phases precipitate once the supersaturation for the phases is achieved. As for our hydrothermal stage, when KOH was used as a mineralizer, part of the nanoclusters was dissolved in an alkali solution under the conditions of high temperature and high pressure. Under the suitable processing condition of hydrothermal treatment, the amorphous phase formed firstly [18]. The amorphous was an intermediate phase to crystalline BLFO phase. As the reaction temperature and time increased, the crystalline BLFO particles were formed by the process of nucleation, precipitation, dehydration, and growth, in the expense of the redissolution of the amorphous owing to their higher free energy than the crystalline phase of the BLFO, corresponding to higher solubility in the same media. In addition, as is well-known, the size and morphology of the product depend strongly on both crystal nucleation and crystal growth, which are determined by pH value of the precursor solution [26]. When KOH concentrations were 5 and 7 M, at the beginning of the crystal growth process, very small particles (∼a few nanometers) were formed, which were usually spherical in shape [27]. These spherical nanoparticles further grew to form spherical microstructure (Fig. 4a and b) when the hydrothermal process was performed at 180 °C for 16 h. If the KOH concentrations further increased up to 9 M and 11 M, the spherical nanoparticles collided to form tile-like particles (Fig. 4c and d). On the other hand, during the hydrothermal process, the sizes of the products were highly dependent on the competition between crystal nucleation and crystal growth [28]. According to our experimental results, a moderately alkaline value (5 and 7 M) resulted in a fast crystal growth that led to a large crystal size (Fig. 4a and b), and a high alkaline value (9 and 11 M) gave rise to a fast nucleation and the formation of a large number of crystal nuclei with small size (Fig. 4c and d).

The discontinue effect of KOH concentration on BFO phase composition has been reported by Cheon et al. [29]. Cheon et al. synthesized multiferroic $BiFeO_3$ powders by hydrothermal method. Their XRD results indicated that with 4 M KOH, crystalline BFO with an impurity phase of a-$Bi_2O_3$was obtained. Using 8 M KOH, a pure BFO phase could be prepared. But, the higher KOH concentration (12 M) was used, besides BFO phase, an impurity phase of bismuth-rich $Bi_{25}FeO_{40}$ was also detected. In our system, the discontinue effect of KOH concentration on BLFO phase composition may be the following factors: First, the phase diagram of Bi_2O_3–Fe_2O_3 was very complex because $Bi_2Fe_4O_9$ and $Bi_{25}FeO_{40}$ were stable compounds surrounding $BiFeO_3$ [6]. Therefore, it is very difficult to precisely control the optimizing conditions for obtaining a single phase multiferroic $BiFeO_3$. Second, according to the literature of Chen et al. [30], in the alkaline hydrothermal conditions, the suitable KOH concentration promoted the formation of Bi–O–Bi bridges between the non-bridging structural hydroxyl groups in the solution. The dissolved Bi^{3+} precursor formed ion group and subsequently Bi_2O_3 crystallites. At the same time, the absorbed Fe^{3+} ions on Bi_2O_3 particles diffused into insolvable Bi_2O_3 to produce precipitations of $Bi_2Fe_4O_9$ and $Bi_{25}FeO_{40}$. As we know, crystal growth only occurred in the region of supersaturated fluid. During this process, under sufficient high temperatures and pressures, the BLFO gel precursor was dissolved in aqueous solution to form an intermediate amorphous phase, and then BLFO nuclei. The concentration of the hydrothermal solution increased with reaction time. Supersaturation was achieved when a sufficient amount of BLFO ions was dissolved in the whole bulk solution. This was crucial because both requirements of supersaturation and stoichiometry for the ions to form BLFO crystallites must be satisfied. If the conditions were carefully maintained during the hydrothermal process, a second phase would not form. Therefore, the dissolution and crystallization process continued in supersaturated fluid in such a way that the system was self-stabilizing. As for specimens synthesized with the KOH concentrations of 7 and 11 M, the amount of KOH was appropriate and beneficial for the formation of pure BLFO. While, when the KOH concentrations were 5 and 9 M, the balance of dissolution and crystallization process for pure BLFO were destroyed because the pH value was changed. At this time, a sufficient amount of component (containing $Bi_2Fe_4O_9$ and $Bi_{25}FeO_{40}$) ions were dissolved in the whole bulk solution, therefore, the supersaturation of $Bi_2Fe_4O_9$ and $Bi_{25}FeO_{40}$ were achieved. Thus, the second phases and irregular grains were detected in XRD patterns and SEM images respectively for specimens synthesized with the KOH concentrations of 5 and 9 M (Figs. 1 and 4).

4. Conclusions

In summary, the pure BLFO microspheres and submicrotiles have been synthesized successfully by the sol–gel-hydrothermal method. In the sol–gel-hydrothermal process, crystal structure, morphology and dimensiona of the BLFO samples strongly depended on KOH concentrations. The hydrothermal conditions created a gentle environment to promote the formation of crystalline BLFO powders at a very low processing temperature of 180 °C, which greatly reduced the synthesized temperature for the BLFO phase in comparison with the conventional sol–gel process by about 500 °C. The sol–gel-hydrothermal route, without the presence of catalysts and expensive equipment, will ensure higher purity in the products and greatly reduce the production cost, and thus offer a novel and simple synthetic route for high-quality ceramics powders.

Acknowledgements

The project was supported by National Natural Science Foundation of China (No. 50702022), the Fundamental Research Funds for the Central Universities, SCUT (No. 2009ZM0015), State Key Laboratory of Pulp and Paper Engineering (South China University of Technology, Nos. 200904, 200901) and State Key Lab of Advanced Technology for Materials Synthesis and Processing (Wuhan University of Technology, No. 2010-KF-4).

References

[1] T. Kimura, S. Kawamoto, I. Yamada, M. Azuma, M. Takano, Y. Tokura, Magnetocapacitance effect in multiferroic $BiMnO_3$, Phys. Rev. B 67 (2003) 180401.
[2] N. Hur, S. Park, P.A. Sharma, J.S. Ahn, S. Guha, S.W. Cheong, Electric polarization reversal and memory in a multiferroic material induced by magnetic fields, Nature 429 (2004) 392–395.
[3] N.A. Spaldin, M. Fiebig, The renaissance of magnetoelectric multiferroics, Science 309 (2005) 391–392.
[4] G.A. Smolenskii, I. Chupis, Ferroelectromagnets, Sov. Phys. Usp. 25 (1982) 475–493.
[5] Y. Chu, Q. Zhan, L.W. Martin, M.P. Cruz, P. Yang, G.W. Pabst, F. Zavaliche, S. Yang, J. Zhang, L. Chen, D.G. Schlom, I. Lin, T. Wu, R. Ramesh, Nanoscale domain control in multiferroic $BiFeO_3$ thin films, Adv. Mater. 18 (2006) 2307–2311.
[6] F. Tyholdt, S. Jorgensen, H. Fjellvag, A.E. Gunnaes, Synthesis of oriented $BiFeO_3$ thin films by chemical solution deposition: phase, texture, and microstructural development, J. Mater. Res. 20 (2005) 2127–2139.
[7] R. Mazumder, P.S. Devi, D. Bhattacharya, P. Choudhury, A. Sen, M. Raja, Ferromagnetism in nanoscale $BiFeO_3$, Appl. Phys. Lett. 91 (2007) 062510.
[8] J.K. Kim, S.S. Kim, W.J. Kim, Sol–gel synthesis and properties of multiferroic $BiFeO_3$, Mater. Lett. 59 (2005) 4006–4009.
[9] S. Kazhugasalamoorthy, P. Jegatheesan, R. Mohandoss, N.V. Giridharan, B. Karthikeyan, R.J. Joseyphus, S. Dhanuskodi, Investigations on the properties of pure and rare earth modified bismuth ferrite ceramics, J. Alloy. Compd. 493 (2010) 569–572.
[10] V.R. Singh, A. Garg, D.C. Agrawal, Structural changes in chemical solution deposited lanthanum doped bismuth ferrite thin films, Appl. Phys. Lett. 92 (2008) 152905.
[11] F. Gao, X.Y. Chen, K.B. Yin, S. Dong, Z.F. Ren, F. Yuan, T. Yu, Z.G. Zou, J.M. Liu, Visible-light photocatalytic properties of weak magnetic $BiFeO_3$ nanoparticles, Adv. Mater. 19 (2007) 2889–2892.
[12] S. Shetty, V.R. Palkar, R. Pinto, Size effect study in magnetoelectric $BiFeO_3$ system, Pramana – J. Phys. 58 (2002) 1027–1230.
[13] S. Ghosh, S. Dasgupta, A. Sen, H.S. Maiti, Low-temperature synthesis of nanosized bismuth ferrite by soft chemical route, J. Am. Ceram. Soc. 88 (2005) 1349–1352.

[14] N. Das, R. Majumdar, A. Sen, H.S. Maiti, Nanosized bismuth ferrite powder prepared through sonochemical and microemulsion techniques, Mater. Lett. 61 (2007) 2100–2104.
[15] J.H. Xu, H. Ke, D.C. Jia, W. Wang, Y. Zhou, Low-temperature synthesis of $BiFeO_3$ nanopowders via a sol–gel method, J. Alloy. Compd. 472 (2009) 473–477.
[16] A.Z. Simões, F.G. Garcia, C.D. Riccardi, Rietveld analysys and electrical properties of lanthanum doped $BiFeO_3$ ceramics, Mater. Chem. Phys. 116 (2009) 305–309.
[17] Y.D. Hou, L. Hou, S.Y. Huang, T.T. Zhang, M.K. Zhu, H. Wang, H. Yan, $(Na_{0.8}K_{0.2})_{0.5}Bi_{0.5}TiO_3$ nanowires: Low-temperature sol–gel-hydrothermal synthesis and densification, J. Am. Ceram. Soc. 90 (2007) 1738–1743.
[18] Z.W. Chen, X.H. He, Low-temperature preparation of nanoplated bismuth titanate microspheres by a sol–gel-hydrothermal method, J. Alloy. Compd. 497 (2010) 312–315.
[19] S.T. Zhang, Y. Zhang, M.H. Lu, C.L. Du, Y.F. Chen, Z.G. Liu, Y.Y. Zhu, N.B. Ming, X.Q. Pan., Substitution-induced phase transition and enhanced multiferroic properties of $Bi_{1-x}La_xFeO_3$ ceramics, Appl. Phys. Lett. 88 (2006) 162901.
[20] A.C. Tas, P.J. Majewski, F. Aldinger, Chemical preparation of pure and strontium- and/or magnesium-doped lanthanum gallate powders, J. Am. Ceram. Soc. 83 (2000) 2954–2960.
[21] X.L. Hu, Y.J. Zhu, Zhu, Morphology control of PbWO4 nano- and microcrystals via a simple, seedless, and high-yield wet chemical route, Langmuir 20 (2004) 1521–1523.
[22] Y.G. Wang, G. Xu, Z.H. Ren, X. Wei, W.J. Weng, P.Y. Du, G. Shen, G.R. Han, Mineralizer-assisted hydrothermal synthesis and characterization of $BiFeO_3$ nanoparticles, J. Am. Ceram. Soc. 90 (2007) 2615–2617.
[23] X.G. Peng, Mechanisms for the shape-control and shape-evolution of colloidal semiconductor nanocrystals, Adv. Mater. 15 (2003) 459–463.
[24] C.R. Peterson, E.B. Slamovich, Effect of processing parameters on the morphology of hydrothermally derived $PbTiO_3$ powders, J. Am. Chem. Soc. 82 (1999) 1702–1710.
[25] P. Pinceloup, C. Courtois, J. Vicens, A. Leriche, B. Thierry, Evidence of a dissolution–precipitation mechanism in hydrothermal synthesis of barium titanate powders, J. Eur. Ceram. Soc. 19 (1999) 973–977.
[26] X. Wang, Y.D. Li, Synthesis and characterization of lanthanide hydroxide single-crystal nanowires, Angew. Chem. Int. Ed. 41 (2002) 4790–4793.
[27] J.T. Han, Y.H. Huang, X.J. Wu, C.L. Wu, W. Wei, B. Peng, W. Huang, J.B. Goodenough, Tunable synthesis of bismuth ferrites with various morphologies, Adv. Mater. 18 (2006) 2145–2148.
[28] E.W. Shi, C.T. Xia, W.Z. Zhong, B.G. Wang, C.D. Feng, Crystallographic properties of hydrothermal barium titanate crystallites, J. Am. Ceram. Soc. 80 (1997) 1567–1572.
[29] S.H. Han, K.S. Kim, H.G. Kim, H.G. Lee, H.W. Kang, J.S. Kim, C.I. Cheon, Synthesis and characterization of multiferroic $BiFeO_3$ powders fabricated by hydrothermal method, Ceram. Int. 36 (2010) 1365–1372.
[30] C. Chen, J.R. Cheng, S.W. Yu, L.G. Che, Z.Y. Meng, Hydrothermal synthesis of perovskite bismuth ferrite crystallites, J. Cryst. Growth 291 (2006) 135–139.